

In Silico Study of Naringenin as Melanogenesis Inducer in Vitiligo

Dian Ardiana^{1,*}, Lestari Dewi², Renata Prameswari¹

Dian Ardiana^{1,*}, Lestari Dewi²,
Renata Prameswari¹

¹Department of Dermatology and
Venereology, Faculty of Medicine, Hang Tuah
University, Surabaya, INDONESIA.

²Department of Pharmacology, Faculty of
Medicine, Hang Tuah University, Surabaya,
INDONESIA.

Correspondence

Dian Ardiana

Department of Dermatology and
Venereology, Faculty of Medicine, Hang
Tuah University, Surabaya, INDONESIA.

E-mail: dian.ardiana@hangtuah.ac.id

History

- Submission Date: 10-08-2022;
- Review completed: 28-09-2022;
- Accepted Date: 20-10-2022.

DOI: 10.5530/pj.2022.14.178

Article Available online

<http://www.phcogj.com/v14/i6>

Copyright

© 2022 Phcogj.Com. This is an open-
access article distributed under the terms
of the Creative Commons Attribution 4.0
International license.

ABSTRACT

Introduction: Vitiligo is a pigmentation disorder characterized by loss of skin color (depigmentation) due to melanocyte dysfunction and loss. Melanocytes produce melanin pigment through a melanogenesis process. Melanocyte survival and melanogenesis process are influenced by Microphthalmia Associated-Transcription Factor (MITF) and several proteins, including WNT, β -catenin, tyrosinase, Tyrosinase-Related Protein-1 (TRP1), and Tyrosinase-Related Protein-2 (TRP2). The current therapy for vitiligo is still unsatisfactory. Naringenin is one of *Rhizophora mucronata* compound, one type of mangrove plant often found in the eastern coastal area of Surabaya City. **Objective:** To investigate the naringenin's potency in melanogenesis and to predict the pharmacokinetics or toxicity of naringenin by in silico study. **Methods:** This is a computational study using a molecular docking method to observe the interaction of naringenin with WNT, β -catenin, MITF, tyrosinase, TRP-1, and TRP-2 proteins. Pharmacokinetic or toxicity prediction of naringenin using the pkCSM method. Psoralen was used as a control. **Results:** Naringenin binds to all these proteins in the same region as psoralen, indicating that naringenin can stimulate melanogenesis. Naringenin has lower binding energy than psoralen on all proteins (except β -catenin), indicating that naringenin's interaction with these proteins is stronger than psoralen. Pharmacokinetic and toxicity predictions show that naringenin has good absorption or permeation, is not mutagenic, is not hepatotoxic, and does not cause skin sensitization. **Conclusion:** This computational study concludes that naringenin has melanogenesis inducer potency and good pharmacokinetics.

Key words: Naringenin, Mangrove, *Rhizophora mucronata*, Vitiligo, WNT.

INTRODUCTION

Vitiligo is a pigmentation disorder characterized by loss of skin color (depigmentation) due to melanocyte dysfunction and loss. The prevalence ranges from 0.5 - 2%. Spots are cosmetically disruptive and have a decreased quality of life.^{1,2} There are several therapeutic strategies for vitiligo, namely reducing melanocyte stress, regulating autoimmune responses, and stimulating melanocyte regeneration,³ all of which aim to stabilize depigmentation and stimulate pigmentation (repigmentation).¹ Therapies include medical (topical, systemic, and phototherapy) as well as surgical,^{4,5} each of which has advantages and disadvantages.^{2,6} After the loss of melanocytes in vitiligo lesions, it is necessary to differentiate, proliferate, and migrate new melanocytes to the epidermis. Nevertheless, it is still a challenge in the field of dermatology.

Melanocytes are cells that produce the pigment melanin, the main determinant of skin, hair, and eye color.¹ Subcellular lysosome-like organelles (melanosomes) inside the melanocytes are responsible for melanogenesis. After melanin is synthesized, along with melanocyte microtubules, the mature melanosomes are transported and transferred to keratinocytes around them. Melanin will then accumulate on top of the keratinocyte nucleus. Tyrosinase-related protein-1 (TRP1), tyrosinase-related protein-2 (TRP2, Dct), and tyrosinase are the enzymes that play a role in melanin synthesis.^{2,7,8}

Wnt, a signaling protein, is known to activate the Wnt/ β catenin pathway⁹ that stimulates melanocyte stem cell differentiation in hair follicles.^{2,10} Signals

generated by Wnt and β -catenin binding stimulate the Microphthalmia-associated transcription factor (MITF) target gene expression in the nucleus. MITF is a major regulatory protein responsible for survival, cell cycle regulation, migration, and differentiation of melanocyte lineages. Therefore, activated MITF will cause melanogenesis.^{7,11} Research on vitiligo lesions treated with Narrow Band UVB phototherapy showed increased Wnt expression in re-pigmented vitiligo lesions around hair follicles (perifollicular),¹² so the Wnt/ β catenin pathway is of concern for the development of vitiligo therapy.

The eastern littoral area of Surabaya City is often grown by *Rhizophora mucronata*.¹³ This plant belongs to the group of *Eukaryota*. The kingdom of this plant is *Plantae*, the phylum is *Spermatophyta*, the subphylum is *Angiospermae*, the class is *Dicotyledonae*, the order is *Rhizophorales*, and the family is *Rhizophoraceae*.¹⁴ The methanol extract of *R. mucronata* leaves showed the content of various ingredients. Those are coumarins (i.e., calophyllic acid, inophyllum C, inophyllum E, isocalophyllic acid, methoxyinophyllum P, calocoumarin B, calophyllolide, and brasimarin C), benzoic acid, flavones (amentoflavone and Naringenin), xanthenes (6-deoxy-jacareubin, jacareubin, 1,3,5-trihydroxy-2-(3-methylbut-2-enyl) xanthone). In addition, two new coumarins and one xanthone have been found.¹⁵

One of the most important naturally occurring flavonoids is naringenin.¹⁶ It is found mostly in some consumable fruits, such as tomatoes and Citrus species, and the *Ficus carica* type Smyrna figs. Naringenin (C₁₅H₁₂O₅), chemically named 2,3-dihydro-5,7-dihydroxy-2-(4-hydroxyphenyl)-4H-1-benzopyran-4-one and exhibits a molecular weight of 272.26. This widely distributed molecule

Cite this article: Ardiana D, Dewi L, Prameswari R. *In Silico* Study of Naringenin as Melanogenesis Inducer in Vitiligo. *Pharmacogn J.* 2022;14(6): 847-855.

is soluble in organic solvents, such as alcohol and insoluble in water. Within the flavonoid class, naringenin is a flavanone derived from the hydrolysis of naringin or narirutin (a glycone precursor). In the flavonoid biosynthetic pathway, Naringenin occupies a central position as a major C15 intermediate.¹⁷ This research is an *in silico* study to investigate whether naringenin from *Rhizophora mucronata* has the potency to induce melanogenesis and can develop a new drug for the treating vitiligo in the future.

MATERIALS AND METHODS

This research is a computational study investigating naringenin's potency and pharmacokinetics/toxicity. Prediction of naringenin's potency in inducing melanogenesis was made by molecular docking. It observed the ligand-protein interaction. This program simulated the binding between naringenin as a ligand to WNT, β -catenin, MITF, tyrosinase, TRP1, and TRP2 protein. Pharmacokinetics, including Absorption, Distribution, Metabolism, Excretion (ADME), and toxicity prediction of naringenin, were done by the pkCSM method.

We downloaded the structure of naringenin (932) from the database of NCBI PubChem.¹⁸ Psoralen (CID 6199) was used as a control, and downloaded from the database of NCBI PubChem. The target protein used were WNT (PDB ID 6AHY), β -catenin (PDB ID 1luj), MITF-M (PDB ID 4ATI), TRP1 (PDB ID 5M8M), TRP2 (PDB ID 1NCI), and tyrosinase (PDB ID 3nq1), which were downloaded from the Protein Data Bank.¹⁹

Docking is done with the Molegro Virtual Docker program version 5.0 on a special area (Grid). The downloaded protein was inputted to the Molegro Virtual Docker 5.0 program and predicted binding cavities (active site of the protein).²⁰ The prediction parameter of binding cavities with a molecular surface is based on a van der Waals force of at least five sides. The active site grid of each protein is: WNT: X= 20.41, Y= -3.68, Z= -25.38, radius 15; β -catenin: X= 30.38, Y= 37.65, Z= 52.31, radius 10; MITF-M: X= -3.19, Y= -7.9, Z= 12.7, radius 11; TRP1: X= -37.59, Y = 31.04, Z = 3.96, radius 15; TRP2: X=19.76, Y=43.82, Z= -41.04, radius 11; Tyrosinase: X= -12.13, Y= -2.31, Z= -8.17, radius 13.

This study uses some other docking parameters. Those are max population size (50); threshold of pose generation energy (100), tries (10-30); max steps of simplex evolution (300); neighbor distance factor (1.00); Number of Runs (10) and Max iteration (1500); MolDock SE algorithm; resolution of grid (0.30); multiple poses number of poses (5); threshold of energy (0.00); cluster similar poses RMSD threshold (1) and Function Moldock Score [Grid]. The program obtained the binding energy of the protein-ligand complex from the total score of the MolDock Score, Moldock Grid, and Rerank score.²⁰ The binding energies are shown in kJ/mol and are from the average of five binding models of the ligand-protein complex. Docking results are visualized in 3D and 2D with the Discovery Studio ver 21.1.1 program. The bond energy value shows the strength of the bond between the receptor and the compound, and the lower bond energy value has a more stable and stronger bond.

RESULTS

Naringenin-WNT complex

Naringenin and psoralen bind to the activator site of WNT protein. It is shown from the 3D view of the compound. The bound residues were ARG195, GLU192, GLU177, ARG176, HIS189, and SER184, while the active sites of psoralen on WNT proteins were ARG183, SER184, ASN187, ASP181, VAL104, PRO103, ARG179, and ARG183. The bonds between naringenin and psoralen with WNT proteins include hydrogen bonds, electrostatics, and hydrophobic interactions. Furthermore, the binding energy of naringenin-WNT is -252.4 kJ/mol, and the binding energy of psoralen-WNT is -243 kJ/mol (Figure 1; Table 1).

Naringenin- β -catenin complex

The Naringenin- β -catenin complex produces bond energy of -213.4 kJ/mol with the active sites bound, including SER473, ASN516, GLU568, GLY512, LYS508, VAL511, and ARG515 (Figure 2; Table 1). Naringenin binds with five hydrogen bonds at residues SER473, ASN516, GLU568, GLY512, and ASN516. In addition, naringenin showed three hydrophobic interactions at residues LYS508, VAL511, and ARG515. The active sites of psoralen bind with β -catenin are GLY572, GLY575, GLU571, ARG515, VAL613, and VAL511. Furthermore, hydrophobic interactions dominate the psoralen- β -catenin interaction. The binding energy of psoralen- β -catenin is -223.8 kJ/mol, and the binding energy of naringenin- β -catenin is -213.4 kJ/mol.

Naringenin-MITF-M complex

The 3D structure of the naringenin-MITF-M and psoralen-MITF-M complexes shows the same binding site. The active site residues bound by naringenin are MET239, ASP252, ALA249, ASP236, TRP241, and LYS233. On the other hand, the active site residues bound by psoralen were ASP236, ALA249, PRO232, ALA249, and LYS256 (Figure 3; Table 1). The amino acid residues bound by the two compounds show that the MITF-M activator site, the binding of naringenin and psoralen on the MITF-M activator site triggers MITF-M for melanogenesis. The bonds formed from naringenin and psoralen to MITF-M proteins are hydrogen bonds, hydrophobic, electrostatic, and unfavorable bonds. Furthermore, naringenin showed a more varied type of bond and bound more amino acid residue. The naringenin-MITF-M binding energy was -196 kJ/mol, and the binding energy of psoralen-MITF-M was -178.4 kJ/mol (Table 1).

Naringenin-TRP1 complex

The 3D structure of the naringenin-TRP1 complex shows the active site at residues ALA67, THR69, PHE105, VAL68, ARG64, PRO446, HIS100, and CYS101. The bond types of the naringenin-TRP1 complex are hydrogen bonding, electrostatic, and hydrophobic interactions (Figure 4; Table 1). Psoralen exhibits three hydrogen bonds. Those are at the amino acid residues ARG64, ARG114, and CYS101. Besides that, there are four hydrophobic interactions at the amino acid residues PRO445, PRO446, CYS101, and PRO445. As a result, naringenin-TRP1 produced a bond energy of -284.2 kJ/mol, and psoralen-TRP1 produced a bond energy of -232.6 kJ/mol.

Naringenin-TRP2 complex

Naringenin binds to the protein TRP2 at the amino acid residues ASN8, GLN19, PRO6, PRO5, GLU20, LEU21, ILE7, and VAL22. Besides hydrogen bonds, the other dominant types of bonds are hydrophobic interactions and van der Waals forces (Figure 5; Table 1). The psoralen bond to TRP2 produces binding energy of -190.8 kJ/mol. Types of bonds that are bound are four hydrogen bonds with active sites ASN8, LEU21, VAL22, and LEU60, two electrostatic bonds at residues, and five hydrophobic interactions at residues ARG23 and PRO6. The naringenin-TRP2 bond was -224.4 kJ/mol.

Naringenin-tyrosinase complex

Naringenin - tyrosinase produces binding energy of -346.8 kJ/mol, with the amino acid residues bound, including GLU141, HIS49, LYS47, ILE139, ALA44, GLY43, PRO52, and ALA40, while the interaction of psoralen - tyrosinase with a binding energy of -268.6 kJ/mol (Figure 6; Table 1). The active sites of psoralen against tyrosinase are LYS47, HIS49, ALA40, PHE48, PRO52, and ILE139.

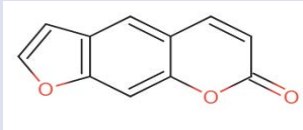
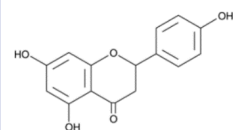
The amount of bond energy, amino acid residues bound, distance, category, and type of bond between compounds and each protein is shown in Table 1.

Table 1: Interaction between naringenin and psoralen on WNT proteins, β -catenin, MITF, TRP1, TRP2, and tyrosinase.

Complex	Binding Energy (kJ/mol)	Interaction	Distance (Å)	Category	Type	
Naringenin-WNT	-252,4	B:ARG195:NH2 - :10:O2	2,52146	Hydrogen Bond	Conventional Hydrogen Bond	
		:10:H10 - B:GLU192:OE1	2,85442			
		:10:H12 - B:GLU177:O	1,98437			
		B:SER184:OG - :10	3,8171	Hydrogen Bond;Electrostatic	Pi-Donor Hydrogen Bond	
		B:HIS189:N - :10	3,48465		Pi-Cation;Pi-Donor Hydrogen Bond	
		:10 - B:ARG176	4,43228		Hydrophobic	Pi-Alkyl
		B:ARG176:NH1 - :10	4,42859		Electrostatic	Pi-Cation
Psoralen-WNT	-243	F:ARG183:NH1 - :10:O3	3,13676	Hydrogen Bond	Conventional Hydrogen Bond	
		F:SER184:OG - :10:O1	2,75032			
		F:ASN187:ND2 - :10:O2	2,69765			
		F:VAL104:N - :10	4,06746	Electrostatic	Pi-Donor Hydrogen Bond	
		F:ASP181:OD2 - :10	4,035		Pi-Anion	
		:10 - F:PRO103	5,35052			
		:10 - F:PRO103	4,42271			
		:10 - F:ARG179	4,61454	Hydrophobic	Pi-Alkyl	
		:10 - F:ARG183	5,05777			
		:10 - F:ARG183	3,99556			
:10 - F:PRO103	4,52678					
:10 - F:ARG183	4,03675					
Naringenin - β Catenin	-213,4	:10:H11 - A:SER473:OG	2,91899	Hydrogen Bond	Conventional Hydrogen Bond	
		:10:H11 - A:ASN516:OD1	2,2479			
		:10:H12 - A:GLU568:O	2,10302			
		A:GLY512:CA - :10:O1	3,22187	Hydrophobic	Carbon Hydrogen Bond	
		A:ASN516:ND2 - :10	3,81875		Pi-Donor Hydrogen Bond	
		:10 - A:LYS508	5,04537			
		:10 - A:VAL511	4,93986		Pi-Alkyl	
:10 - A:ARG515	5,24246					
Psoralen - β Catenin	-223,8	A:GLY572:CA - :10	3,11232	Hydrophobic	Pi-Sigma	
		A:GLY575:CA - :10	3,38639			
		A:GLU571:C,O;GLY572:N - :10	3,77576	Hydrophobic	Amide-Pi Stacked	
		A:GLU571:C,O;GLY572:N - :10	4,32169			
		:10 - A:ARG515	4,94797			
		:10 - A:ARG515	4,7407		Pi-Alkyl	
:10 - A:VAL613	5,02984					
:10 - A:VAL511	5,42511					
Naringenin-MITF-M	-196	B:MET239:N - :10:O5	3,07507	Hydrogen Bond	Conventional Hydrogen Bond	
		:10:H10 - B:ASP252:OD2	1,61668			
		:10:H11 - B:ALA249:O	2,38899			
		:10:H12 - B:ASP236:O	2,23883	Electrostatic	Pi-Cation	
		B:ASP236:N - :10	4,99065		Other	Pi-Lone Pair
		B:ASP236:O - :10	2,93495		Pi-Sigma	
		B:ALA249:CB - :10	3,41452			
		B:TRP241 - :10	4,50316	Hydrophobic	Pi-Pi T-shape	
		B:TRP241 - :10	4,14613			
		:10 - B:LYS233	5,22881		Pi-Alkyl	
:10 - B:MET239	4,43978					
B:TRP241:HZ2 - :10:C9	1,41766	Unfavorable	Unfavorable Bump			
Psoralen-MITF-M	-178,4	B:ASP236:OD2 - :10	4,82133	Electrostatic	Pi-Anion	
		B:ASP236:OD2 - :10	4,1713			
		B:ALA249:CB - :10	3,47134		Pi-Sigma	
		:10 - B:PRO232	4,51496	Hydrophobic		
		:10 - B:PRO232	4,50534		Pi-Alkyl	
		:10 - B:ALA249	4,65052			
:10 - B:LYS256	4,52427					

Complex	Binding Energy (kJ/mol)	Interaction	Distance (Å)	Category	Type
Naringenin - TRP1	-284,2	:10:H10 - B:ALA67:O	2,4559	Hydrogen Bond	Conventional Hydrogen Bond
		:10:H11 - B:THR69:O	2,14328		
		:10:H12 - B:PHE105:O	2,24723		
		B:VAL68:CA - :10:O3	2,97852	Electrostatic	Carbon Hydrogen Bond
		A:ARG64:NH2 - :10	3,61281		Pi-Cation
		B:PRO446:CB - :10	3,69706		Pi-Sigma
		B:HIS100 - :10	4,99037		Pi-Pi T-shaped
:10 - B:CYS101	4,82793	Hydrophobic	Pi-Alkyl		
Psoralen - TRP1	-232,6	A:ARG64:NH2 - :10:O1	2,63814	Hydrogen Bond	Conventional Hydrogen Bond
		B:ARG114:NH1 - :10:O3	2,69838		Pi-Donor Hydrogen Bond
		B:CYS101:N - :10	4,05056		
		:10 - B:PRO445	5,05698	Hydrophobic	Pi-Alkyl
		:10 - B:PRO446	4,47982		
:10 - B:CYS101	4,15247				
:10 - B:PRO445	5,42754				
Naringenin - TRP2	-224,4	B:ASN8:ND2 - :10:O2	3,22362	Hydrogen Bond	Conventional Hydrogen Bond
		B:GLN19:NE2 - :10:O5	2,6924		
		:10:H10 - B:PRO6:O	2,03193		
		:10:H11 - B:PRO5:O	2,23078		
		:10:H12 - B:GLU20:O	1,99965	Hydrophobic	Carbon Hydrogen Bond
		:10:H1 - B:ASN8:O	2,97962		
		:10 - B:LEU21	4,59767		
		:10 - B:ILE7	4,32385		
:10 - B:VAL22	5,22403				
Psoralen - TRP2	-190,8	A:ASN8:ND2 - :10:O3	2,8646	Hydrogen Bond	Conventional Hydrogen Bond
		B:LEU21:N - :10:O1	2,95543		
		B:VAL22:N - :10:O1	3,08802		
		:10:H5 - B:LEU60:O	2,72094	Electrostatic	Carbon Hydrogen Bond
		B:GLU20:OE1 - :10	3,63963		Pi-Anion
		B:GLU20:OE1 - :10	4,05808		
		B:VAL22:C,O;ARG23:N - :10	3,52435	Hydrophobic	Amide-Pi Stacked
		B:VAL22:C,O;ARG23:N - :10	3,90076		
		:10 - B:ARG23	4,91924		
:10 - B:ARG23	4,68796	Pi-Alkyl			
:10 - A:PRO6	4,53057				
Naringenin - Tyrosinase	-351,4	:10:H10 - B:GLU141:O	2,10964	Hydrogen Bond	Conventional Hydrogen Bond
		:10:H12 - A:HIS49:O	2,03954		
		A:LYS47:NZ - :10	4,01392	Hydrogen Bond;Electrostatic	Pi-Cation;Pi-Donor Hydrogen Bond
		B:ILE139:CD1 - :10	3,63437		Pi-Sigma
		B:GLY43:C,O;ALA44:N - :10	4,55336		Amide-Pi Stacked
		:10 - A:PRO52	5,3035	Hydrophobic	Pi-Alkyl
		:10 - B:ALA40	4,53942		
		:10 - A:LYS47	4,95244		
:10 - B:ALA40	4,85125				
:10 - B:ALA44	5,11897				
Psoralen - Tyrosinase	-268,6	A:LYS47:NZ - :10:O3	3,13	Hydrogen Bond	Conventional Hydrogen Bond
		A:HIS49:N - :10:O1	2,94716		
		:10:H5 - A:HIS49:O	2,4383		
		B:ALA40:CB - :10	3,86977	Hydrophobic	Carbon Hydrogen Bond
		A:PHE48 - :10	4,97181		Pi-Sigma
		:10 - A:PHE48	4,03359		Pi-Pi Stacked
		:10 - A:PRO52	4,9067	Hydrophobic	Pi-Alkyl
		:10 - B:ALA40	4,85926		
		:10 - B:ILE139	4,57923		
:10 - B:ILE139	4,49325				
:10 - B:ALA40	4,05971				

Table 2: Molecular description of naringenin and psoralen.

	Psoralen	Naringenin
Molecule depiction (SMILES)		
MW	186.166	272.256
LogP	2.5392	2.5099
SA	78.555	114.235
RB	0	1
Donors	0	3
Acceptors	3	5

MW = Molecular Weight, RB =Rotatable Bonds, SA = Surface Area

Table 3: Predicted pharmacokinetics and toxicity of naringenin.²¹

Property	Model Name	Predicted Value	
		Psoralen	Naringenin
Absorption	Solubility to water	-2.474 log mol/L	-3.224 log mol/L
	Permeability to Caco2	1.295 log Papp in 10 cm/s	1.029 log Papp in 10 cm/s
	Intestinal absorptions (in human)	96.668 %	91.31 %
	Permeability to skin	-2.216 log Kp	-2.742 log Kp
	P-glycoprotein I and II inhibitor	No	No
	P-glycoprotein substrate	Yes	Yes
Distribution	VDss (in human)	-0.13 log L/kg	-0.015 log L/kg
	Fraction unbound (in human)	0.301 Fu	0.064 Fu
	Permeability to BBB	0.41 log BB	-0.578 log BB
	Permeability to CNS	-1.714 log PS	-2.215 log PS
Metabolism	CYP2D6/CYP3A4 substrate	No	No
	CYP1A2 inhibitors	Yes	Yes
	CYP2C19/CYP2C9/CYP2D6/CYP3A4 inhibitor	No	No
	Clearance Total	0.773 log ml/min/kg	0.06 log ml/min/kg
Excretion	OCT2 substrate renal	No	No
	Toxicity AMES	No	No
Toxicity	Max. tolerated dose (in humans)	-0.253 log mg/kg/day	-0.176 log mg/kg/day
	hERG I/ hERG II inhibitor	No	No
	Toxicity for Oral Rat Acute (LD50)	1.874 mol/kg	1.791 mol/kg
	Toxicity for Oral Rat Chronic (LOAEL)	1.07 log mg/kg BW/day	1.944 log mg/kg_bw/day
	Hepatotoxicity	No	No
	Skin Sensitisation	No	No
	<i>T. Pyriformis</i> toxicity	0.524 log ug/L	0.369 log ug/L
	Minnow toxicity	1.334 log mM	2.136 log mM

Prediction results of pharmacokinetics and toxicity using the pkCSM naringenin method and when compared with psoralen are:

DISCUSSION

This computational study showed that naringenin and psoralen bind to the activator site of WNT protein. The same bound residue was SER184. The binding energy of naringenin-WNT is lower than psoralen-WNT. This result indicates that naringenin is stronger than the complex formed in psoralen-WNT. The active site of β -catenin was bound to both naringenin and psoralen. The same bound residue was VAL515. Naringenin binds with five hydrogen bonds and three hydrophobic

interactions. Hydrophobic interactions dominate psoralen- β -catenin interaction. The binding energy of naringenin- β -catenin is higher than psoralen- β -catenin. This finding indicates that naringenin is weaker than the complex formed in psoralen- β -catenin. Naringenin and psoralen bind to the MITF-M active site. The same bound residues were ALA249 and ASP236. Naringenin had a more varied type of bond and bound more amino acid residues. Naringenin-MITF-M binding energy is lower than psoralen-MITF-M. This result indicates that naringenin is stronger than the complex formed in psoralen-MITF-M. Naringenin and psoralen bind to the TRP1 active site. The same bound residues were ARG64, CYS101, and PRO446.

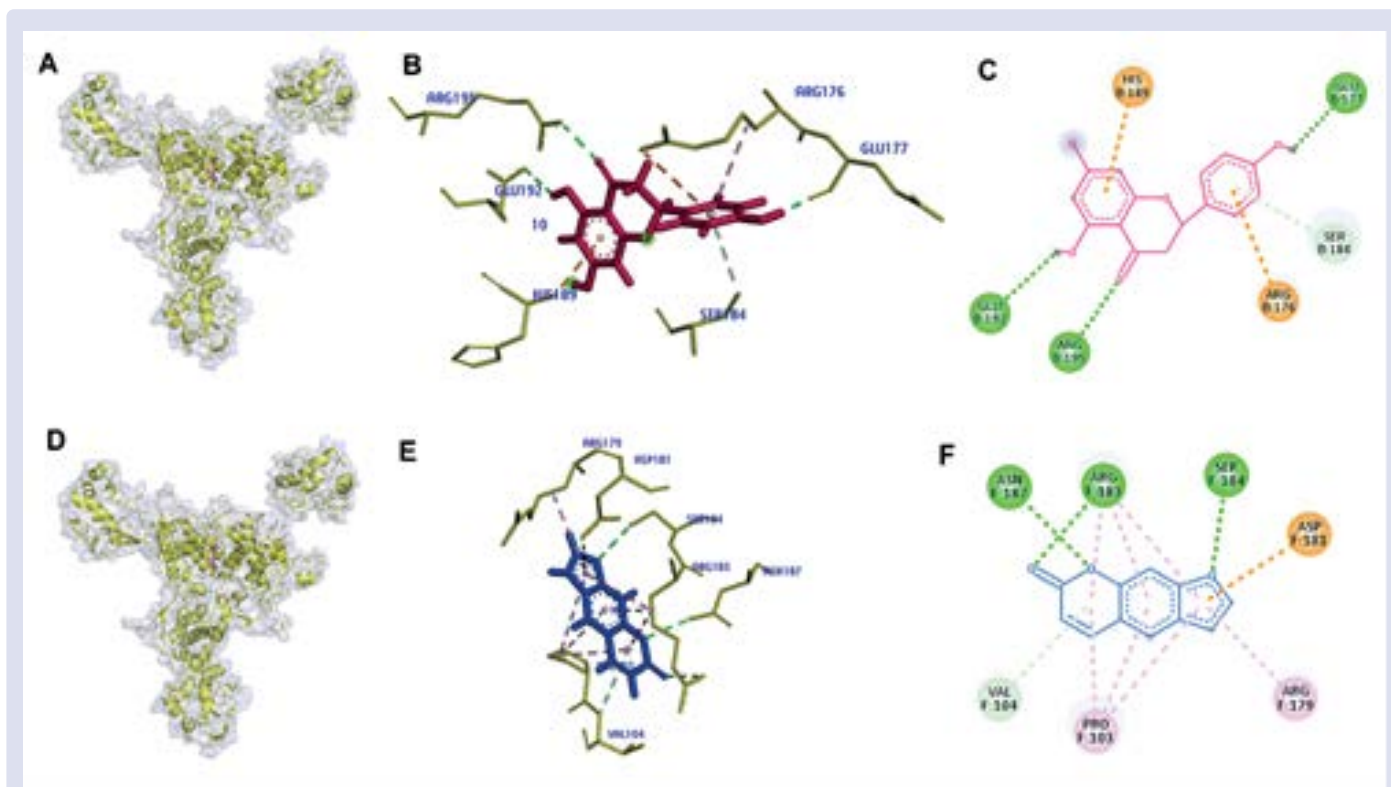


Figure 1: Interaction between naringenin and psoralen with WNT protein, A-C complex of naringenin-WNT, D-F complex of psoralen-WNT.

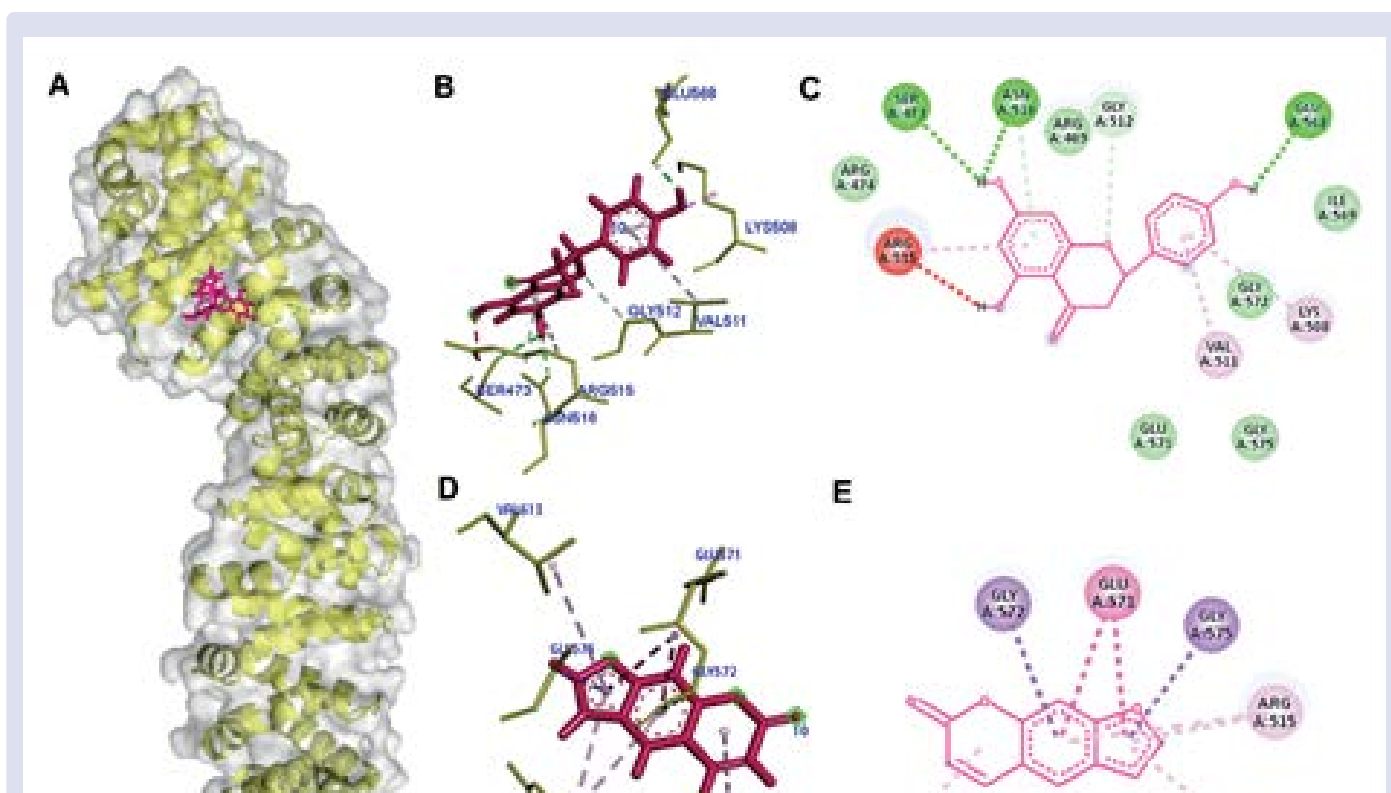


Figure 2: Interaction of naringenin and psoralen with β -catenin, A. Superimposed ligand-protein binding complex, B. 3D view of the naringenin- β -catenin complex, C. 2D view of the naringenin- β -catenin complex, D. 3D view of the psoralen- β -catenin complex, E. 2D view of the psoralen- β -catenin complex, yellow color indicates protein, pink indicates compound.

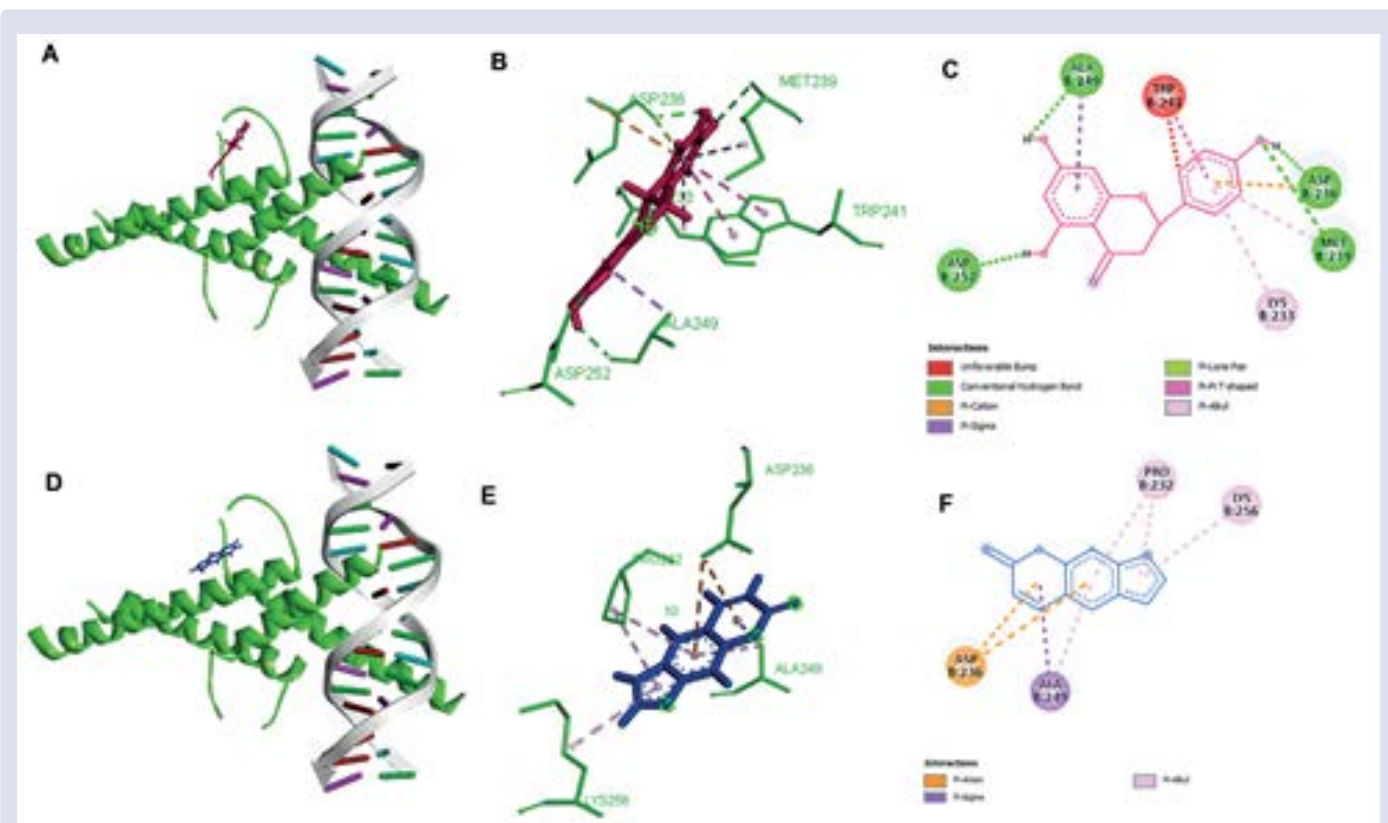


Figure 3: Interaction between naringenin and psoralen with MITF-M protein, A-C complex of naringenin-MITF-M, D-F complex of psoralen-MITF-M.

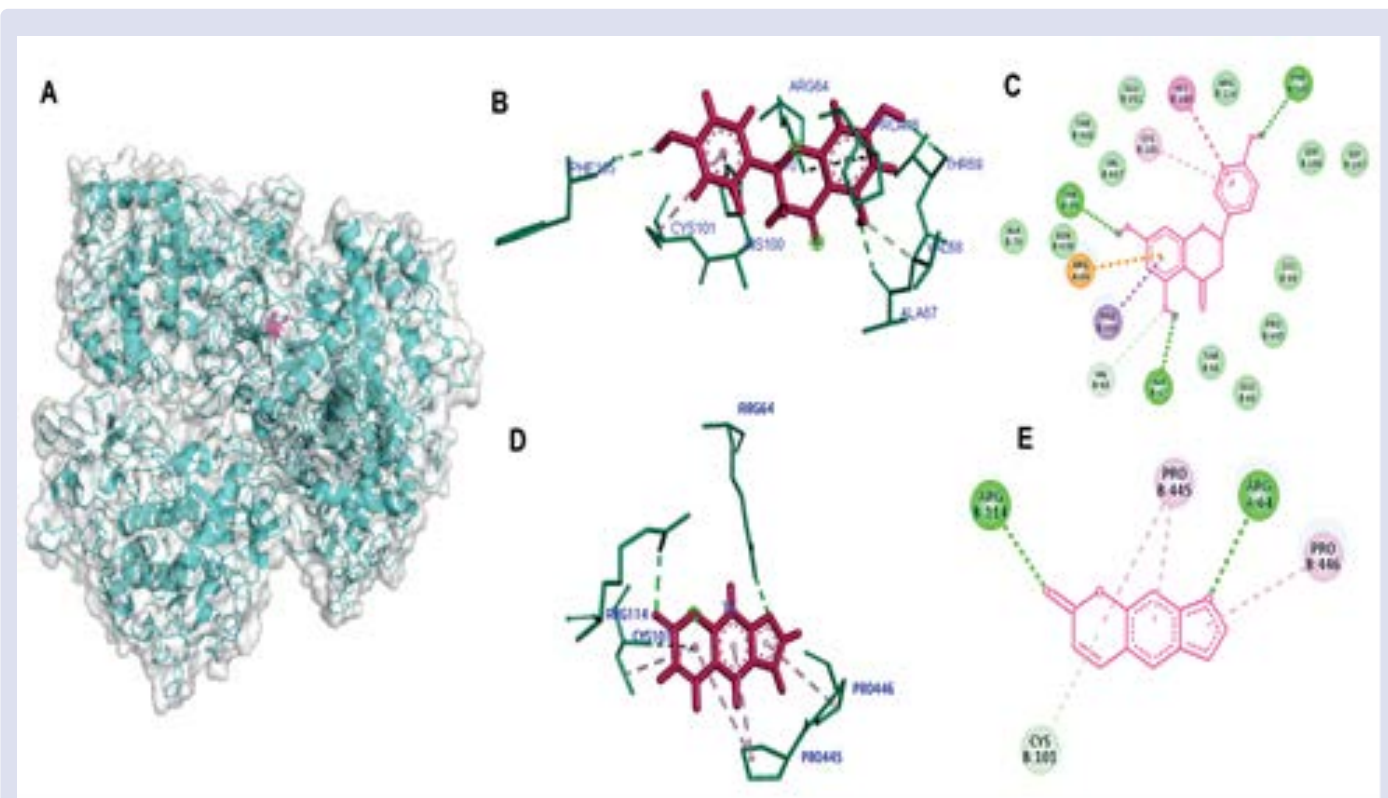


Figure 4: Interaction of naringenin and psoralen with TRP1. A. Superimposed ligand-protein binding complex, B. 3D view of the naringenin-TRP1 complex, C. 2D view of the naringenin-TRP1 complex, D. 3D view of the psoralen-TRP1 complex, E. 2D view of the psoralen-TRP1 complex. Tosca shows TRP1 protein, and pink indicates compound.

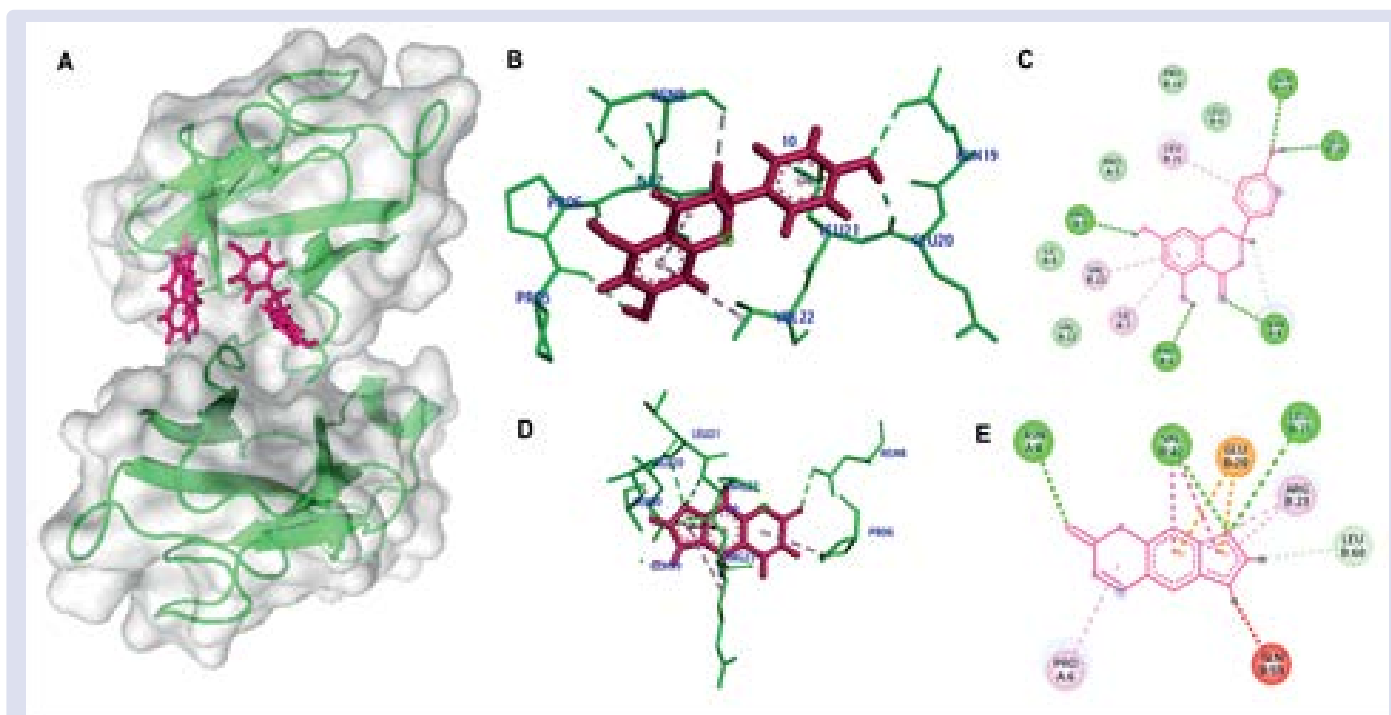


Figure 5: Interaction of naringenin and psoralen with TRP2, A. Superimposed ligand-protein binding complex, B. 3D view of the naringenin-TRP2 complex, C. 2D view of the psoralen-TRP2 complex, E. 2D view of the psoralen-TRP2 complex, color tosca shows TRP2 protein, pink indicates compound.

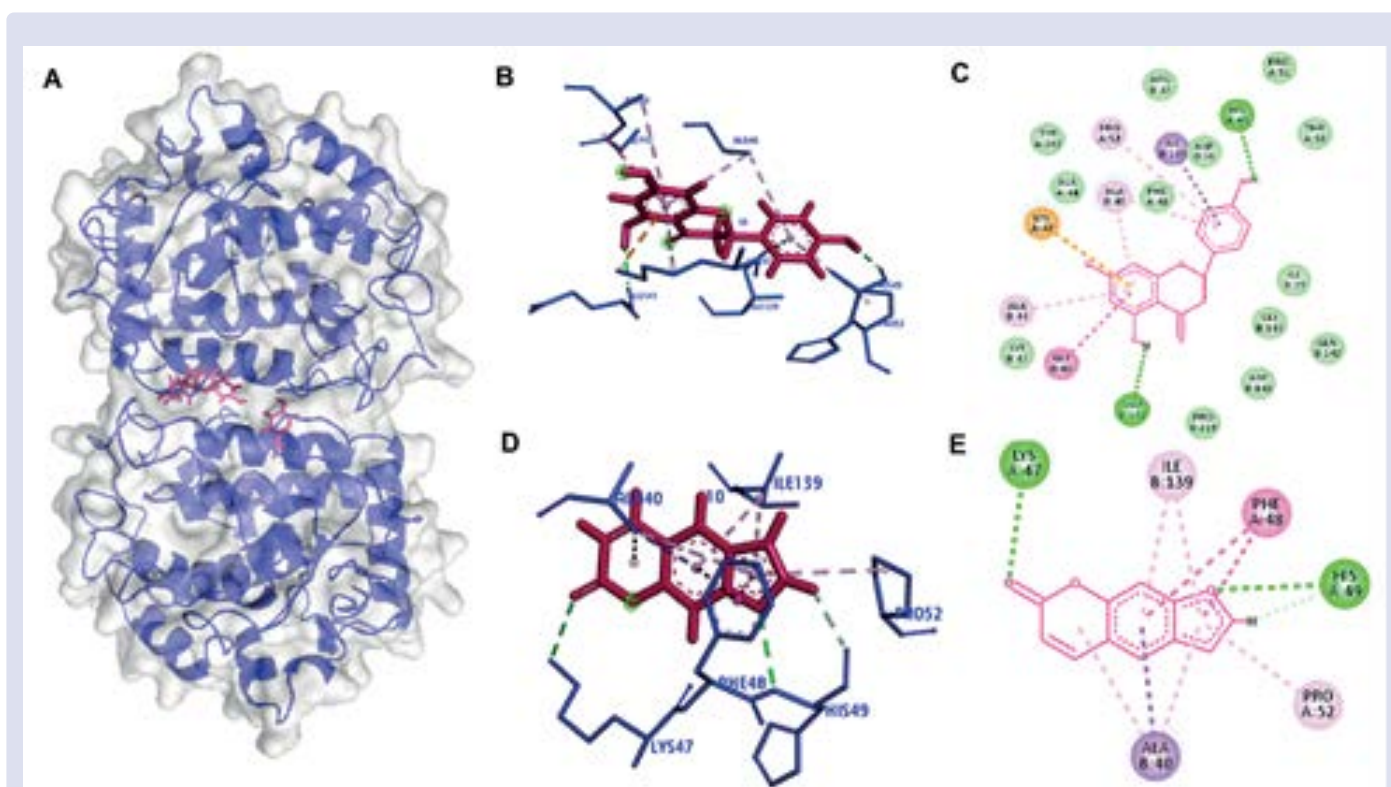


Figure 6: Interaction between naringenin and psoralen with tyrosinase, A. Superimposed ligand-protein binding complex, B. 3D view of the naringenin-tyrosinase complex, C. 2D view of the naringenin-tyrosinase complex, D. 3D view of the psoralen-tyrosinase complex, E. 2D psoralen-tyrosinase complex. Blue indicates a tyrosinase protein, and pink indicates a compound.

Naringenin-TRP1 produced bond energy lower than psoralen-TRP1, which indicates that naringenin is stronger than the complex formed in psoralen-TRP1. Naringenin and psoralen bind to the TRP2 active site. The same bound residue was ASN8, LEU21, VAL22, and PRO6. Naringenin-TRP2 binding energy was lower than the psoralen-TRP2 bond. This result indicates that naringenin is stronger than the complex formed in psoralen-TRP2. Naringenin and psoralen bind to the tyrosinase active site. The same bound residues were LYS47, HIS49, ALA40, and ILE139. Naringenin-tyrosinase binding energy was lower than the psoralen-tyrosinase bond. This result indicates that naringenin is stronger than the complex formed in psoralen-tyrosinase.

Prediction of poor absorption of a material is seen from 5 things (the rule of 5), namely if there are more than ten Hydrogen bond acceptors (viewed from the number of Ns and Os), more than five Hydrogen bond donors (viewed from the number of OHs and NHs), the molecular weight is more than 500, and the calculated Log P (CLogP) is more than 5 (or MLogP > 4.15).²²⁻³⁰ Naringenin, like psoralen, has a good prediction of absorption or permeation.

Predictive analysis of pkCSM in absorption shows that:

Naringenin has a better predictive value of solubility to water than psoralen (more soluble in water than psoralen)

The permeability of Caco-2 is high when the value is > 0.9. Naringenin and psoralen have Caco-2 permeability > 0.9, so they can penetrate the intestinal mucosa easily. Naringenin showed good intestinal absorption (in humans) because the predictive value was > 30%.

Naringenin has a skin permeability predictive value of -2.742 (lower than -2.5 log Kp) which indicates that naringenin has higher permeability than psoralen, making it more easily absorbed by the skin.

P-glycoprotein is a transporter. It works as a biological barrier by removing toxins and xenobiotics. Naringenin is predicted to act as a substrate for P-glycoprotein.

Predictive analysis of pkCSM in distribution shows that:

The volume of distribution in plasma is said to be high if more than 2.81 L/kg (log VDss > 0.45) and low if less than 0.71 L/kg (log VDss < -0.15). Therefore, naringenin has a low volume of distribution; thus, a carrier is needed when given orally.

The unbound fraction of naringenin is less than that of psoralen. This low unbound fraction makes naringenin less efficient at penetrating cell membranes.

The Blood Brain Barrier (BBB) penetration is considered easy if the BB log > 0.3 and bad if the BB log < -1. The central nervous system penetration is said to be difficult/not penetrate if the log PS < -3 and easy if the log PS > -2. Psoralen penetrates the BBB and the central nervous system more easily than naringenin.

Predictive analysis of pkCSM in metabolism shows that:

Naringenin, like psoralen, is predicted to act as an inhibitor of the CYP1A2 (cytochrome P450) enzyme. It makes the enzyme unable to work so that drugs metabolized through the cytochrome P450 pathway have a more prolonged effect.

Predictive analysis of pkCSM in excretion shows that:

Total naringenin clearance is 0.06 log ml/min/kg. Naringenin does not work as a substrate for OCT2 (transporter in the kidney).

Predictive analysis of pkCSM in toxicity indicates that:

Naringenin does not have AMES toxicity (not mutagenic), does not have hepatotoxic properties, and does not cause skin sensitization.

This study shows that naringenin can stimulate the process of melanogenesis. Further research needs to be done because some phenolic compounds are known to act as tyrosinase inhibitors so that melanin formation does not occur.^{31,32}

CONCLUSION

This study concluded that naringenin binds to WNT, β -Catenin, MITF-M, TRP1, TRP2, and tyrosinase, in the same region as psoralen. It indicates that naringenin has a melanogenesis inducer potency. Naringenin showed lower bond energy to WNT, MITF-M, TRP1, TRP2, and tyrosinase proteins than psoralen. It indicated that naringenin's interaction with these proteins was stronger than psoralen. Pharmacokinetics and toxicity predictions of naringenin showed that naringenin has a good absorption or permeation. It did not have a mutagenic effect, hepatotoxic, and did not cause skin sensitization. Further studies, *in vitro* and *in vivo*, are needed to know the effect of naringenin *Rhizophora mucronata*.

CONFLICTS OF INTEREST

We have no conflicts of interest.

SOURCE OF FUNDING

This study was supported by the Faculty of Medicine – Hang Tuah University.

ACKNOWLEDGMENTS

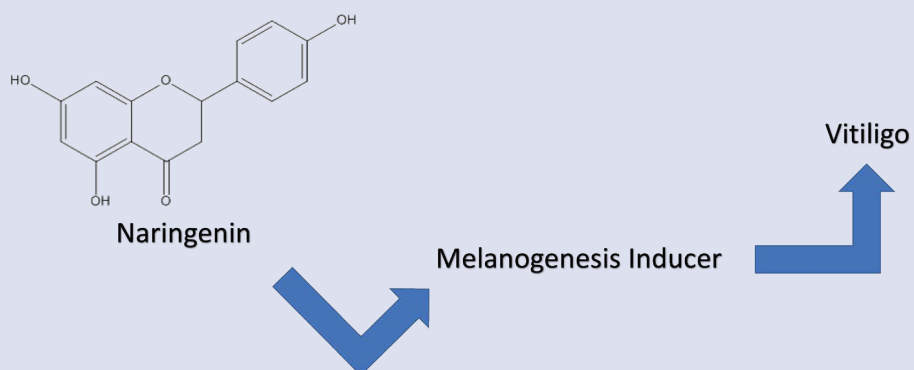
We thank EJA Team, Indonesia for editing the manuscript.

REFERENCES

- Bergqvist C, Ezzedine K. Vitiligo: A Review. *Dermatol*. 2020;236(6):571-92.
- Abdel-Malek ZA, Jordan C, Ho T, Upadhyay PR, Fleischer A. The official journal of International Federation of Pigment Cell Societies Society for Melanoma Research. The enigma and challenges of vitiligo pathophysiology and treatment. *Pigment Cell Melanoma Res*. 2020;33(6):778-7.
- Vaniary TIN, Listiawan MY, Murtiastutik D. Expression of Melan-A in Depigmented Skin of Vitiligo Patients. *Berkala Ilmu Kesehatan Kulit Dan Kelamin*. 2020;32(1):17-20.
- Razmi TM, Parsad D. Recent Advances in Pathogenesis and Medical Management of Vitiligo. *Pigmentary skin Dis*. 2018;123-38.
- Lee J, Kwon HS, Jung HM, Lee H, Kim GM, Yim HW. Treatment Outcomes of Topical Calcineurin Inhibitor Therapy for Patients with Vitiligo: A Systematic Review and Meta-analysis. *JAMA Dermatol*. 2019;155(8):929-38.
- Karagaiah P. Emerging drugs for the treatment of vitiligo. *Expert Opin Emerg Drugs*. 2020;25(1):7-24.
- Nguyen NT, Fisher DE. MITF and UV responses in skin : From pigmentation to addiction. *Pigment Cell Melanoma Res*. 2019;32(2):224-36.
- Kang HY, Suzuki I, Lee DJ, Ha J, Reiniche P, Aubert J, et al. Transcriptional Profiling Shows Altered Expression of Wnt Pathway– and Lipid Metabolism–Related Genes as Well as Melanogenesis-Related Genes in Melasma. *J Invest Dermatol*. 2011;131(8):1692-700.
- Huang P, Yan R, Zhang X, Wang L, Ke X, Qu Y. Activating Wnt/ β -catenin Signaling Pathway for Disease Therapy: Challenges and Opportunities. *Jpt. Pharmacol Ther*. 2019;196:79-90.
- Guo H, Xing Y, Liu Y, Luo Y, Deng F, Yang T, et al. Wnt/ β -catenin signaling pathway activates melanocyte stem cells in vitro and in vivo. *J Dermatol Sci*. 2016;83(1):45-51.

11. Yamada T, Hasegawa S, Inoue Y, Date Y, Arima M, Yagami A, et al. Comprehensive analysis of melanogenesis and proliferation potential of melanocyte lineage in lentigo solaris. *J Dermatol Sci.* 2014;73(3):251-7.
12. Ardiana D. Expression of WNT1 signaling proteins after phototherapy exposure in vitiligo. *J Pak Assoc Derma.* 2019;29(3):302-8.
13. Irawanto R. Keanekaragaman Vegetasi Mangrove di Pesisir Kota Surabaya Dan Potensinya Sebagai Fitoremediator Lingkungan', in *Prosiding Seminar Nasional Biologi di Era Pandemi COVID-19 Gowa.* 2020.
14. Datasheet CABI (<https://www.cabi.org/isc/datasheet/47510>).
15. Taniguchi K. Two new coumarins and a new xanthone from the leaves of *Rhizophora mucronata*. *Bioor Med. Chem Lett.* 2018;28(6):1063-6.
16. Rao PV, Kiran SDVS, Rohini P, Bhagyasree P. Flavonoid: A review on Naringenin. *J Pharmacogn Phytochem.* 2017;6(5):2778-83.
17. Salehi B. The therapeutic potential of naringenin: A review of clinical trials. *Pharmaceuticals.* MDPI AG. 2019.
18. Database PubChem NCBI (<https://pubchem.ncbi.nlm.nih.gov/compound/>)
19. Protein Data Bank (<https://www.rcsb.org/>)
20. Bitencourt-Ferreira G, de Azevedo WFJ. Molegro Virtual Docker for Docking.', *Methods in molecular biology* (Clifton, N.J.). The United States. *Methods Mol Biol.* 2019;2053:149-67.
21. Pires DEV, Blundell TL, Ascher DB. pkCSM: Predicting small-molecule pharmacokinetic and toxicity properties using graph-based signatures. *J Med Chem.* 2015;58(9):4066-72.
22. Lipinski CA, Lombardo F, Dominy BW, Feeney PJ. Experimental and computational approaches to estimate solubility and permeability in drug discovery and development settings. *Adv Drug Deliv Rev.* 2001;46(1-3):3-26.
23. Ansori ANM, Kharisma VD, Solikhah TI. Medicinal properties of *Muntingia calabura* L.: A Review. *Res J Pharm Technol.* 2021;14(8):4509-2.
24. Fadholly A, Ansori ANM, Sucipto TH. An overview of naringin: Potential anticancer compound of citrus fruits. *Res J Pharma Technol.* 2020;13(11):5613-9.
25. Kharisma VD, Probojati RT, Murtadlo AAA, Ansori ANM, Antonius Y, Tamam MB. Revealing Potency of Bioactive Compounds as Inhibitor of Dengue Virus (DENV) NS2B/NS3 Protease from Sweet Potato (*Ipomoea batatas* L.) Leaves. *Indian J Forensic Med Toxicol.* 2020;15(1):1627-32.
26. Widyananda MH, Pratama SK, Samoedra RS, Sari FN, Kharisma VD, Ansori ANM, et al. Molecular docking study of sea urchin (*Arbacia lixula*) peptides as multi-target inhibitor for non-small cell lung cancer (NSCLC) associated proteins. *J Pharm Pharmacogn Res.* 2021;9(4):484-96.
27. Kharisma VD, Agatha A, Ansori ANM, Widyananda MH, Rizky WC, Dings TGA, et al. Herbal combination from *Moringa oleifera* Lam. And *Curcuma longa* L. as SARS-CoV-2 antiviral via dual inhibitor pathway: A viroinformatics approach. *J Pharm Pharmacogn Res.* 2022;10(1):138-46.
28. Wijaya RM, Hafidzhah MA, Kharisma VD, Ansori ANM, Parikesit AP. COVID-19 In Silico Drug with *Zingiber officinale* Natural Product Compound Library Targeting the Mpro Protein. *Makara J Sci.* 2021;25(3):5.
29. Antonius Y, Utomo DH, Widodo. Identification of potential biomarkers in nasopharyngeal carcinoma based on protein interaction analysis. *Int J Res Appl.* 2017;13(4):376-88.
30. Ongko J, Setiawan JV, Feronytha AG, Juliana A, Effraim A, Wahjudi M, et al. In-silico screening of inhibitor on protein epidermal growth factor receptor (EGFR). *IOP Conference Series: Earth Env Sci.* 2022;1041:012075.
31. Panzella L, Napolitano A. Natural and Bioinspired Phenolic Compounds as Tyrosinase Inhibitors for the Treatment of Skin Hyperpigmentation: Recent Advances. *Cosmetics.* 2019;6(4):57.
32. Fan M, Ding H, Zhang G, Hu X, Gong D. Relationships of dietary flavonoid structure with its tyrosinase inhibitory activity and affinity. *LWT - Food Science and Technol.* 2019;107:25-34.

GRAPHICAL ABSTRACT



ABOUT AUTHORS



Dr. Dian Ardiana, Sp.KK. is a lecturer at the Department of Dermatology and Venereology, Faculty of Medicine, Hang Tuah University, Surabaya, Indonesia.

Cite this article: Ardiana D, Dewi L, Prameswari R. *In Silico* Study of Naringenin as Melanogenesis Inducer in Vitiligo. *Pharmacogn J.* 2022;14(6): 847-855.